Unified unquenched quark model for heavy-light mesons with chiral dynamics

Ru-Hui Ni,[1] Jia-Jun Wu,[2,3,*] and Xian-Hui Zhong[1,4,†]

[1]*Department of Physics, Hunan Normal University, and Key Laboratory of Low-Dimensional Quantum Structures and Quantum Control of Ministry of Education, Changsha 410081, China*
[2]*School of Physical Sciences, University of Chinese Academy of Sciences (UCAS), Beijing 100049, China*
[3]*Southern Center for Nuclear-Science Theory (SCNT), Institute of Modern Physics, Chinese Academy of Sciences, Huizhou 516000, Guangdong Province, China*
[4]*Synergetic Innovation Center for Quantum Effects and Applications (SICQEA), Hunan Normal University, Changsha 410081, China*

(Received 16 October 2023; accepted 6 May 2024; published 10 June 2024)

In this work, an unquenched quark model is proposed for describing the heavy-light mesons by taking into account the coupled-channel effects induced by chiral dynamics. After including a relativistic correction term for the strong transition amplitudes, both the mass spectra and decay widths of the observed heavy-light mesons can be successfully described simultaneously in a unified framework, several long-standing puzzles related to the small masses and broad widths are overcome naturally. We also provide valuable guidance in searching new heavy-light mesons by the detailed predictions of their masses, widths, and branching ratios. The success of the unquenched quark model presented in this work indicates it may be an important step for understanding the hadron spectrum.

DOI: 10.1103/PhysRevD.109.116006

I. INTRODUCTION

The fundamental theory of strong interaction is quantum chromodynamics (QCD). One of its most prominent challenges is the phenomenon of confinement, the elementary systems we observe, known as hadrons and composed of quarks and gluons, appear to be colorless. In the low-energy regime, the nonperturbative effects make it impossible to achieve analytical computations. Lattice QCD simulation can provide the hadronic spectra from first principles, but it falls short of offering a detailed picture of hadrons. In such circumstances, a theoretical model becomes essential for gaining a deeper insight into the nature of confinement.

The quenched quark model, initially based solely on $q\bar{q}$ for mesons and qqq for baryons and developed in the 1960s by Gell-Mann and Zweig [1–3], effectively described the hadron spectrum until the discovery of the $X(3872)$ [4] and $D_s(2317)$ in 2003 [5]. Over the past two decades, an increasing number of hadron states, often referred to as "exotic," have been observed [6]. These discoveries, including the XYZ and P_c states, have challenged the predictions of the simple $q\bar{q}$ and qqq models [7,8]. An undeniable factor contributing to this discrepancy is the omission of coupled-channel effects resulting from hadron loops in these quark models. This deficiency has long been recognized and discussed, for instance in 1980, when a similar effect known as the meson cloud was proposed [9]. This underscores the importance of considering interactions at both the quark (gluon) level and the hadron level to obtain a comprehensive understanding of physical hadrons.

The significance of coupled-channel effects is widely acknowledged within the scientific community. However, conducting a systematic study in practical calculations presents several challenging issues. The primary concerns can be summarized as follows:

P1. How to select the coupled-channels.
P2. How to obtain correct both mass and width.
P3. How to evaluate the coupled channel effects in the high momentum region.

All of these challenges add complexity when employing a comprehensive model. Consequently, existing research has primarily focused on exploring coupled-channel effects for states that deviate significantly from conventional quark models, rather than those with well-established explanations within the hadron spectrum. For instance, while considering loop contributions for scalar mesons, such as

*wujiajun@ucas.ac.cn
†zhongxh@hunnu.edu.cn

$K\bar{K}$ and $\pi\pi$ loops, only quark level interactions are accounted for ρ meson where the $\pi\pi$ loop indeed significantly shifts the mass of ρ. This lack of consistency and self-consistency within the theory arises as an issue. Furthermore, in the context of strong decay, many studies have been conducted on several phenomenological models, however, the widths of higher resonances are hard to accurately described [7,8].

In the past 20 years, numerous excited heavy-light meson candidates have been observed by collaborations such as D0, CDF, *BABAR*, and LHCb [6], which bring good opportunities for theoretical studies. There are many discussions of the heavy-light meson spectrum based on various quenched quark models [10–32]. In this work, beyond the quenched framework, we introduce a unified unquenched quark model framework that accounts for coupled-channel effects induced by chiral dynamics, utilizing a semi-relativistic potential to interpolate both the masses and widths of all heavy-light mesons. Although there are many attempts based on the unquenched quark model framework, most theoretical studies have primarily focused on near-threshold heavy-light states, such as $D_{s0}^*(2317)$ and $D_{s1}(2460)$ [33–38], or have been limited to the D_s spectrum or D spectrum separately [39–41]. In comparison to the mass spectrum, $D_0(2550)/D_{s0}(2590)$ and $D_1^*(2600)/D_{s1}^*(2700)$ can be categorized as radial excitations. However, the predicted decay widths within the chiral quark model [26–31] are systematically smaller than the observed values. Thus, a comprehensive investigation of both the mass spectra and decay widths for all heavy-light mesons, including D, D_s, B, and B_s mesons, within a unified framework that incorporates unquenched coupled-channel effects is currently lacking. This is a crucial step in the development of a comprehensive model for hadron physics.

The paper is organized as follows. In Sec. II, we give an introduction to the unquenched framework. In Secs. III and IV, the mass spectrum and widths for the heavy-light mesons obtained within the unquenched framework are reported. Then, in Sec. V, some predictions for the missing heavy-light meson resonances are given. Finally, a summary is given in Sec. VI.

II. FRAMEWORK

In the unquenched quark model including coupled-channel effects, as described in previous works [41–44], the Hamiltonian of the hadronic system is described by

$$\mathcal{H} = \mathcal{H}_0 + \mathcal{H}_c + \mathcal{H}_I. \tag{1}$$

Here, $\mathcal{H}_0$ represents the Hamiltonian governing the bare $Q\bar{q}$ state denoted as $|A\rangle$, and it is derived from the semirelativistic quark potential model. $\mathcal{H}_c$ is the noninteracting Hamiltonian for the continuum state $|BC\rangle$, while $\mathcal{H}_I$ is an effective Hamiltonian for describing the coupling between $|A\rangle$ and $|BC\rangle$. The quark (gluon) level interactions are all encompassed within $\mathcal{H}_0$, which are clearly defined, as introduced in the Appendix.

In the coupled-channel model [41–44] the mass of a dressed hadron is estimated by

$$M = M_A + \Delta M(M), \tag{2}$$

where M_A is the bare mass determined by the $\mathcal{H}_0$, while $\Delta M(M)$ stands for the hadronic mass shift, which is given by

$$\Delta M(M) = \mathrm{Re}\sum_{BC}\int_0^\infty \frac{\overline{|\mathcal{M}_{A\to BC}(\boldsymbol{q})|^2}}{(M - E_{BC})} q^2 dq. \tag{3}$$

Here, $\overline{|\mathcal{M}_{A\to BC}(\boldsymbol{q})|^2} \equiv \int \overline{|\langle BC,\boldsymbol{q}|\mathcal{H}_I|A\rangle|^2} d\Omega_{\boldsymbol{q}}$, $\boldsymbol{q} \equiv (0,0,q)$, and E_{BC} is the kinematic energy of the $|BC,\boldsymbol{q}\rangle$ continuum state with the loop momentum $\boldsymbol{q}$.

In principle, all hadronic loops should contribute a mass shift to the bare hadron. However, it is unfeasible to calculate the self-energy function including an unlimited number of loops. To address the question posed in *P1* on the first page, in our calculations, we included all Okubo-Zweig-Iizuka (OZI)-allowed two-body hadronic channels with mass thresholds below the bare states. The contributions from the other virtual channels are subtracted from the dispersion relation by redefining the bare mass with the once-subtracted method suggested in Ref. [45]. In the following, we give a brief introduction to this approach. By introducing a subtracted term $\Delta M(M_0)$ at some suitable point $M = M_0$, the Eq. (2) can be rewritten as

$$M = [M_A + \Delta M(M_0)] + [\Delta M(M) - \Delta M(M_0)]. \tag{4}$$

Since $\Delta M(M)$ will be effectively constant for those virtual channels of a hadron resonance, their contributions will cancel out in

$$\Delta M(M, M_0) = \Delta M(M) - \Delta M(M_0). \tag{5}$$

Consequently, the mass-shift $\Delta M(M, M_0)$ is entirely contributed by the fully opened hadronic channels. Combining Eq. (3), one can explicitly express $\Delta M(M, M_0)$ by

$$\begin{aligned}\Delta M(M, M_0) &= \mathrm{Re}\sum_{BC}\int_0^\infty \frac{\overline{|\mathcal{M}_{A\to BC}(\boldsymbol{q})|^2}}{(M - E_{BC})} q^2 dq \\ &\quad - \mathrm{Re}\sum_{BC}\int_0^\infty \frac{\overline{|\mathcal{M}_{A\to BC}(\boldsymbol{q})|^2}}{(M_0 - E_{BC})} q^2 dq, \\ &= \mathrm{Re}\sum_{BC}\int_0^\infty \frac{(M_0 - M)\overline{|\mathcal{M}_{A\to BC}(\boldsymbol{q})|^2}}{(M - E_{BC})(M_0 - E_{BC})} q^2 dq.\end{aligned} \tag{6}$$

Generally, a ground state, which is lower than the threshold of the first OZI-allowed channel is chosen as a subtraction point M_0. In this case, the subtracted term $\Delta M(M_0)$ [i.e., the second term in Eq. (6)] is entirely contributed by the virtual channels and approximately a constant. Thus, $\Delta M(M_0)$ can be absorbed into the bare mass through a redefinition. Then, the physical mass of a hadron resonance is estimated by

$$M = M_A + \Delta M(M, M_0), \tag{7}$$

when we adopt the once-subtracted method. In our calculations of the $D_{(s)}$ and $B_{(s)}$ spectra, the subtraction points M_0 are set at the corresponding ground states. This method has been applied to study the coupled-channel effects on D/D_s meson states and charmonium states in the literature [39,46]. It should be emphasized that the application of the once-subtracted method is a crucial step for obtaining a successful description of the heavy-light meson spectrum within a unified unquenched quark model.

For a strong decay process $A \to BC$, the partial decay width is obtained by

$$\Gamma = 2\pi \frac{|\boldsymbol{q}| E_B E_C}{M} \overline{|\mathcal{M}_{A\to BC}(\boldsymbol{q})|^2}, \tag{8}$$

where $\boldsymbol{q}$ and $E_{B/C}$ are the on-shell momentum and energy of particle B/C in the decay, respectively.

The central challenge lies in the evaluation of the strong transition amplitude $\langle BC, \boldsymbol{q}|\mathcal{H}_I|A\rangle$. This amplitude can be determined by using the chiral quark model incorporating chiral dynamics [47], as outlined in previous works [26–32,48–50]. In the chiral quark model, the low-energy quark-antiquark-pseudoscalar-meson interaction is described by the chiral Lagrangian,

$$\mathcal{L}_P = \sum_j \frac{1}{f_m} \bar{\psi}_j \gamma_\mu^j \gamma_5^j \psi_j \vec{\tau} \cdot \partial^\mu \vec{\phi}_m. \tag{9}$$

Here, ψ_j represents the jth quark field in the hadron, ϕ_m is the pseudoscalar meson field, τ is an isospin operator, and f_m is the pseudoscalar meson decay constant.

In the calculation of the strong transition amplitude $\langle BC, \boldsymbol{q}|\mathcal{H}_I|A\rangle$, we adopt the nonrelativistic wave functions obtained from the potential model Hamiltonian $\mathcal{H}_0$ for the initial and final heavy-light meson states. To match the nonrelativistic form of the wave functions, one should provide a nonrelativistic form of the quark-pseudoscalar meson coupling described by Eq. (9). By carrying out a nonrelativistic reduction, one can obtain the nonrelativistic form at the tree level in the center-of-mass system of the initial hadron, which is given by

$$\mathcal{H}_I = \mathcal{H}_I^{NR} + \mathcal{H}_I^{RC}, \tag{10}$$

where $\mathcal{H}_I^{NR}$ as the nonrelativistic term up to the $1/m$ order is given by [49,50]

$$\mathcal{H}_I^{NR} = g \sum_j \left[\mathcal{G} \boldsymbol{\sigma}_j \cdot \boldsymbol{q} + \frac{\omega_m}{2\mu_q} (\boldsymbol{\sigma}_j \cdot \boldsymbol{p}_j) \right] I_j \varphi_m, \tag{11}$$

while $\mathcal{H}_I^{RC}$ as a relativistic correction term at the mass order of $1/m^2$ is given by [51,52]

$$\mathcal{H}_I^{RC} = -\frac{g}{32\mu_q^2} \sum_j [m_{\mathbb{P}}^2 (\boldsymbol{\sigma}_j \cdot \boldsymbol{q}) + 2\boldsymbol{\sigma}_j \cdot (\boldsymbol{q} - 2\boldsymbol{p}_j) \times (\boldsymbol{q} \times \boldsymbol{p}_j)] I_j \varphi_m. \tag{12}$$

It should be mentioned that to properly derive the relativistic correction term $\mathcal{H}_I^{RC}$, the FWT transformation [53–56] for the chiral Lagrangian given in Eq. (9) is performed. In the electromagnetic interaction, a similar term of $\mathcal{H}_I^{RC}$ appears as the spin-orbit coupling in the relativistic correction [57]. In Eqs. (11) and (12), $\boldsymbol{p}_j$ and $\boldsymbol{\sigma}_j$ are the internal momentum operator and the spin operator of the jth light quark in a hadron, respectively. $\varphi_m = e^{-i\boldsymbol{q}\cdot\boldsymbol{r}_j}$ is the plane wave part of the emitted light meson with three-vector momentum and energy denoted by $(\boldsymbol{q}, \omega_m)$. $m_{\mathbb{P}}$ stands for the mass of the light pseudoscalar meson. I_j is an isospin operator defined in the SU(3) flavor space [49]. The factors g and $\mathcal{G}$ are defined by $g \equiv \delta\sqrt{(E_i + M_i)(E_f + M_f)}/f_m$ and $\mathcal{G} \equiv -(1 + \frac{\omega_m}{E_f + M_f} + \frac{\omega_m}{2m'_j})$, respectively. Here, δ is a global parameter that accounts for the strength of quark-meson couplings. E_i and M_i (E_f and M_f) are the energy and mass of the initial (final) heavy hadron, respectively. μ is defined by $1/\mu = 1/m_j + 1/m'_j$, where m_j and m'_j are the masses of the jth light quark in the initial and final heavy hadrons, respectively. Finally, it should be pointed out that the $1/m^3$ or higher power terms of the quark-pseudoscalar-meson coupling operator only appear in the loop diagrams. For example, at the one-loop level, the quark-pseudoscalar-meson coupling operator will be strongly suppressed by the factor $(\delta \frac{q}{4\pi f_m})^3 = (\delta \frac{q}{\Lambda_{\chi SB}})^3$, where q represents derivatives acting on the pseudoscalar-meson fields, and $\Lambda_{\chi SB} = 4\pi f_m$ is the chiral symmetry breaking scale [47].

It is noteworthy that $\mathcal{H}_I^{RC}$ has often been overlooked in the existing literature [26–32,48–50,58–71]. However, the recent investigations of the strong decays of baryons [51,52] have underscored the significance of $\mathcal{H}_I^{RC}$. In this work, we will include this term within the meson sector, and we will illustrate its pivotal role in accurately determining the widths of mesons. This effectively addresses the *P2* concern, especially the correct width, raised on the first page.

As we know the vertices described by $\mathcal{H}_I$ are only effective in the nonperturbative region, which reflects the

ability of $q\bar{q}$ creation in the vacuum. This ability will be suppressed in the high momentum region due to the weak interactions between the valence quarks. To suppress the nonphysical contributions in the high-momentum region due to the hard vertices given by the chiral quark model, as indicated in *P3*, we incorporate a suppressed factor $e^{-\boldsymbol{q}^2/(2\Lambda^2)}$ into the transition amplitude,

$$\langle BC, \boldsymbol{q}|\mathcal{H}_I|A\rangle \to \langle BC, \boldsymbol{q}|\mathcal{H}_I e^{-\frac{\boldsymbol{q}^2}{2\Lambda^2}}|A\rangle, \tag{13}$$

as that done in the literature [72–76]. In fact, a similar suppressed factor $\sqrt{\Lambda^2/(\Lambda^2+\boldsymbol{q}^2)}$ is widely adopted in the study of the hadron spectrum and hadron-hadron interactions within the chiral constituent quark model [10,77–81]. The cutoff parameter Λ determines the scale at which chiral symmetry is broken. The typical range of Λ is about 0.8 ± 0.2 GeV. We should emphasize that the application of suppressed factor is another crucial step for obtaining a successful description of the correct masses for the heavy-light mesons within a unified unquenched quark model as the *P2* concern. With this method, the mass corrections contributed by the higher partial wave couplings can be controlled.

Within this framework, we systematically address the significant issues *P1–P3* outlined on the first page as follows.

III. SPECTRUM

In Fig. 1, we present a comprehensive heavy-light meson spectrum across three distinct models alongside existing experimental data. The crossing points showing the spectrum including the coupled-channel effects are much closer to the experimental data than the results of other models. This improvement is further illustrated by the significant reduction in the magnitude of χ^2, defined as $\sum_i(\mathrm{Thy}(i)-\mathrm{Exp}(i))^2/\mathrm{Error}(i)^2$. The details of the numerical values of the mass spectrum are given in Tables I. Based on these results, there is no doubt that the coupled channels play a key role in interpolating the spectra of the heavy-light mesons.

First, the coupled-channel effects show their most significant influence on the $^3P_0$ and P_1 states. This is due to their strong couplings to *S*-wave interactions, involving a pseudo-scalar-heavy-meson and a vector-heavy-meson with a pseudo-scalar-light-meson for $^3P_0$ and P_1 states, respectively, which can be seen in Tables III and IV of the Appendix. For instance, there are strong interactions between $D_{s0}^*(2317)$ and DK, as well as between $D_{s1}(2460)$ and D^*K. These substantial coupled-channel effects naturally account for the significant mass shifts observed in these positive parity states. In contrast, the other two positive parity states, P_1' and $^3P_2$, which involve *D*-wave interactions with the coupled channels,

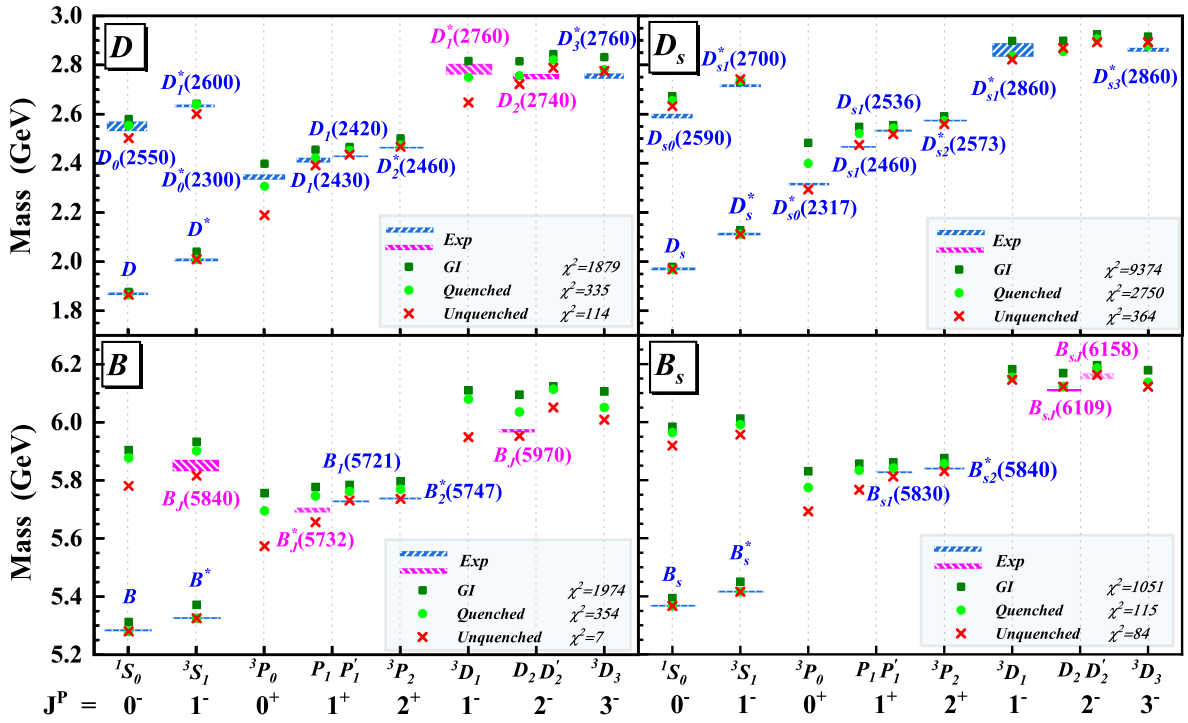

FIG. 1. Mass spectra of heavy-light mesons compared with the observations. The $\chi^2 = \sum_i(\mathrm{Thy}(i)-\mathrm{Exp}(i))^2/\mathrm{Error}(i)^2$ for the well-known GI model, our quenched model and unquenched spectrum, respectively. Here Thy, Exp, and Error represent the theoretical results, experimental data, and error, respectively. It should be noted that for data with experimental errors less than 1 MeV, we unified set Error = 2 MeV because our systemic error should be larger than several MeV.

TABLE I. Theoretical masses and widths compared with the data. The mass spectra from both the quenched and unquenched pictures are given, which are denoted with Q and UQ, respectively. The strong decay widths, which combine the unquenched spectra and are described by nonrelativistic chiral interactions $\mathcal{H}_I^{NR}$, are further augmented by a relativistic correction term $\mathcal{H}_I^{RC}$. These widths are denoted as Γ_i^{NR} and Γ_i^{NR+RC}, respectively. The experimental data are taken from the particle data group (PDG) [6]. The mixing angles for $1P_1/1P_1'$ states in the D, D_s, B, and B_s families are determined to be $-30.0°$, $-26.5°$, $-34.3°$, and $-34.2°$, respectively. While the mixing angles for $1D_2/1D_2'$ states in the D, D_s, B, and B_s families are determined to be $-40.5°$, $-40.5°$, $-39.9°$, and $-40.2°$, respectively. It should be pointed out that in our estimations of the decay widths for the $1P_1$ and $1P_1'$ states, the mixed angle $-54.7°$ extracted in the heavy quark limit has been adopted, the reason was discussed in our previous work [31]. The bold numbers in the table represent the masses and widths of the selected states for determining the parameters.

	D mesons							*D_s mesons*						
		Mass (MeV)			Width (MeV)				Mass (MeV)			Width (MeV)		
$n^{2S+1}L_J$	Observed state	Q	UQ	*Exp*	Γ_i^{NR}	Γ_i^{NR+RC}	*Exp*	Observed state	Q	UQ	*Exp*	Γ_i^{NR}	Γ_i^{NR+RC}	*Exp*
1^1S_0	D^0	**1865**	**1865**	1865	⋯	⋯	⋯	D_s	**1969**	**1969**	1969	⋯	⋯	⋯
1^3S_1	D^*	**2010**	**2009**	2008	0.0529	0.0121	< 2.1	D_s^*	**2112**	**2112**	2112	⋯	⋯	⋯
				2010	0.1294	0.0252	0.0834							
2^1S_0	$D_0(2550)$	2554	2503	2549 ± 19	38	**233**	165 ± 24	$D_{s0}(2590)$	2655	2633	2591 ± 9	11	66	89 ± 20
2^3S_1	$D_1^*(2600)$	2640	2601	2627 ± 10	50	**134**	141 ± 23	$D_{s1}^*(2700)$	2738	2743	2714 ± 5	17	93	122 ± 10
1^3P_0	$D_0^*(2300)$	**2307**	**2189**	2343 ± 10	154	284	229 ± 16	$D_{s0}^*(2317)$	**2400**	**2294**	2318	⋯	⋯	< 3.8
$1P_1$	$D_1(2430)$	**2422**	**2392**	2412 ± 9	120	309	314 ± 29	$D_{s1}(2460)$	2522	2475	2460	⋯	⋯	< 3.5
$1P_1'$	$D_1(2420)$	**2453**	**2436**	2422.1 ± 0.6	19.2	10.7	31.3 ± 1.9	$D_{s1}(2536)$	**2544**	**2519**	2535	0.6	0.3	0.92 ± 0.05
1^3P_2	$D_2^*(2460)$	**2475**	**2468**	$2461.1^{+0.7}_{-0.8}$	45.2	34.5	47.3 ± 0.8	$D_{s2}^*(2573)$	**2574**	**2560**	2569	18.4	13.4	16.9 ± 0.7
1^3D_1	$D_1^*(2760)$?	2750	2648	2781 ± 22	116	103	177 ± 40	$D_{s1}^*(2860)$	2838	2823	2859 ± 27	42	21	159 ± 80
$1D_2$	$D_2(2740)$	2757	2723	2747 ± 6	104	159	88 ± 19	⋯	2855	2870	⋯	29	25	⋯
$1D_2'$	⋯	2822	2789	⋯	59	49	⋯	⋯	2907	2893	⋯	24	19	⋯
1^3D_3	$D_3^*(2750)$	**2782**	**2776**	2763 ± 3	39	33	66 ± 5	$D_{s3}^*(2860)$	**2879**	**2893**	2860 ± 7	27	22	53 ± 10

	B mesons							*B_s mesons*						
		Mass (MeV)			Width (MeV)				Mass (MeV)			Width (MeV)		
$n^{2S+1}L_J$	Observed state	Q	UQ	*Exp*	Γ_i^{NR}	Γ_i^{NR+RC}	*Exp*	Observed state	Q	UQ	*Exp*	Γ_i^{NR}	Γ_i^{NR+RC}	*Exp*
1^1S_0	B^0	**5280**	**5280**	5280	⋯	⋯	⋯	B_s	**5367**	**5367**	5367	⋯	⋯	⋯
1^3S_1	B^*	**5325**	**5325**	5325	⋯	⋯	⋯	B_s^*	**5416**	**5416**	5416	⋯	⋯	⋯
2^1S_0	⋯	5877	5781	⋯	35	289	⋯	⋯	5964	5919	⋯	16	125	⋯
2^3S_1	$B_J(5840)^+$?	5902	5816	5851 ± 19	19	296	224 ± 104	⋯	5991	5957	⋯	6	162	⋯
1^3P_0	⋯	**5695**	**5573**	⋯	153	283	⋯	⋯	**5775**	**5693**	⋯	⋯	⋯	⋯
$1P_1$	$B_J^*(5732)$?	5746	5656	5698 ± 8	149	315	128 ± 18	⋯	5834	5767	⋯	⋯	⋯	⋯
$1P_1'$	$B_1(5721)^0$	**5762**	**5731**	5726.1 ± 1.3	24.6	13.3	27.5 ± 3.4	$B_{s1}(5830)$	5842	5813	5829	0.05	0.03	0.5 ± 0.4
1^3P_2	$B_2^*(5747)^0$	**5769**	**5736**	5739.5 ± 0.7	35.0	23.0	24.2 ± 1.7	$B_{s2}^*(5840)$	5857	5831	5840	2.18	1.57	1.49 ± 0.27
1^3D_1	⋯	6080	5949	⋯	143	141	⋯	⋯	6154	6146	⋯	82	40	⋯
$1D_2$	$B_J(5970)^0$?	6036	5953	5971 ± 5	97	99	81 ± 12	$B_{sJ}(6109)$?	6123	6122	6108.8 ± 1.8	63	31	22 ± 9
$1D_2'$	⋯	6114	6051	⋯	84	81	⋯	$B_{sJ}(6158)$?	6186	6163	6158 ± 9	33	32	72 ± 43
1^3D_3	⋯	6051	6009	⋯	47	35	⋯	⋯	6137	6122	⋯	25	26	⋯

have minor mass shifts. This statement is consistent with the findings in Refs. [73,82]. The mass of $D_0^*(2300)$ with $J^P = 0^+$, which is approximately 2189 MeV in our results, is notably lower than the experimental value of 2343 ± 10 MeV [6]. However, the mass of $D_0^*(2300)$ remains a subject of debate in various theoretical studies [83–87], primarily because its line shape cannot be explained by the Breit-Wigner form used in the experimental analysis for extracting its mass. Notably, lattice QCD calculations are consistent with our findings, where the complex pole position of D_0^* state is at $M - i\Gamma/2 = 2200 - i200$ MeV [88]. The $B_J(5732)$ listed in the Review of Particle Physics [6] maybe favor the broad mixed state $B_1(1P_1)$. With this assignment, the measured mass $M_{\rm exp} = 5698$ MeV and

width $\Gamma_{\rm exp} = 128 \pm 18$ MeV for the $B_J(5732)$ are comparable with the quark model predictions.

Second, the ground states of pseudoscalars and vectors with $J^P = 0^-, 1^-$ exhibit minimal changes across all model for a small coupled-channel effect, because their low mass forbids the decay channels except D^* which also has a very small width. Conversely, the radial excited states have substantial mass shifts. The vector-heavy-meson and pseudoscalar channels will couple with these excited states in P wave, while for the D and B case, additional positive parity heavy-meson and pseudoscalar channels can also coupled with them in S wave. Consequently, the mass shifts are even larger in the D and B cases.

Third, let us consider $1D$-wave heavy-light meson states. It is interesting to note that in the D_s and B_s sectors, the mass shifts are negligible, while they are significant in the D and B sectors. Actually, for the excited D_s and B_s states, the pionic decay is prohibited due to isospin conservation, while K meson is too heavy to effectively couple with positive parity excited D or B states in S wave. As a result, for D_s and B_s sectors, the coupled-channel effects predominantly involve interactions with higher partial waves. In contrast, S-wave channels remain available for D and B excited states when coupled with positive parity excited D and B states and pion. It is natural to interpolate the large mass shift in D and B sectors for $1D$-wave states. It should be mentioned that there is a significant mass shift for the $D(1^3D_1)$ state due to a strong S-wave coupling to the $D_1(2420)\pi$ channel. The physical mass of this $J^P = 1^-$ state is predicted to be about 2650 MeV, which lies about 50 MeV above the other vector state $D_1^*(2600)$. If considering the $D_1^*(2760)$ resonance observed in the $D^+\pi^-$ channel at LHCb [89] as the $D(1^3D_1)$ assignment, then the measured mass $M_{\rm exp} = 2781 \pm 22$ MeV is too large to be comparable with our prediction within the unquenched quark model, although it is consistent with that of the quenched picture. The existence of $D_1^*(2760)$ requires to be further confirmed in future experiments, which may be useful to test the unquenched quark model.

IV. WIDTH

With the parameter set of the unquenched quark model for the mass spectrum, we can further compute the strong decay widths for all heavy-light meson resonances. In Fig. 2, we present the widths with and without $\mathcal{H}_I^{RC}$ by the red crossing and green circle points, respectively. The numerical values compared with the data are also collected in Table I. More details of the strong decay properties can be found in Tables III and IV of the Appendix. The widths of all well-established heavy-light meson states can be globally described well by including the relativistic correction term $\mathcal{H}_I^{RC}$.

From Fig. 2, it is seen that for the radially excited states 2^1S_0 and 2^3S_1 across all heavy-light mesons, the widths are

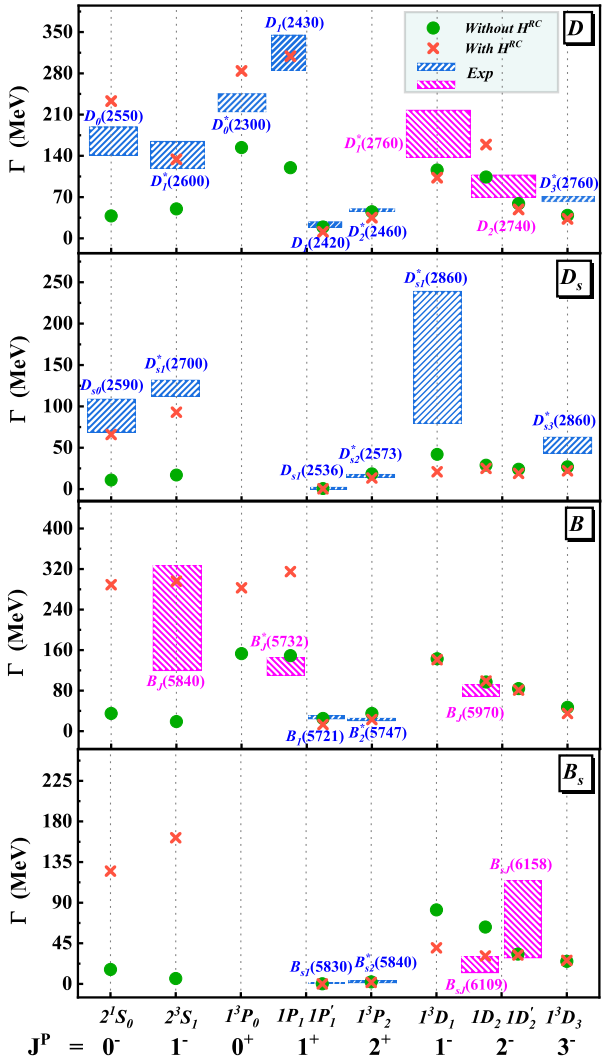

FIG. 2. Predictions of strong decay widths for the heavy-light mesons compared with the observations [6]. The cross (circular) symbol represents the predictions of the width with (without) the incorporation of the relativistic term $\mathcal{H}_I^{RC}$ by combining unquenched spectra.

enhanced significantly by including $\mathcal{H}_I^{RC}$. This naturally addresses a long-standing puzzle, a broad width of $D_0(2550)/D_{s0}(2590)$ and $D_1^*(2600)/D_{s1}^*(2700)$ in chiral quark model studies [27–31]. For $D_1^*(2600)$, the predicted partial width ratio $R_{th}^{D\pi/D^*\pi} = \Gamma(D\pi)/\Gamma(D^*\pi) \simeq 0.28$ is in good agreement with the data $R_{\rm exp}^{D\pi/D^*\pi} = 0.32 \pm 0.11$ [6]. Additionally, for the $^3P_0$ and P_1' in D and B sectors, the widths also exhibit increasing, which leads to the predicted widths of $D_0^*(2300)$ and $D_1(2430)$ are both closer to the observations.

Finally, we give a brief explanation of the enhancement mechanism for the radially excited heavy-light mesons by including the relativistic corrections. For $\mathcal{H}_I^{NR}$ of order $1/m$, the matrix elements of the $\sigma_j \cdot \boldsymbol{q}$ and $\sigma_j \cdot \boldsymbol{p}_j$ terms have a comparable magnitude and cancel out each other, which

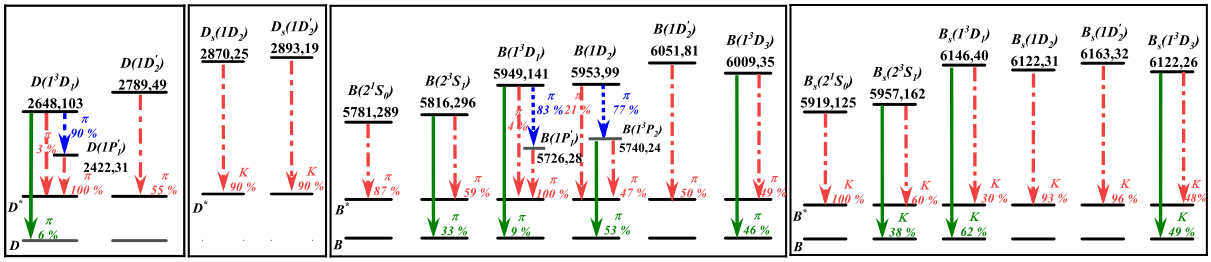

FIG. 3. Predictions of decay rates of the main decay channels for the missing or unwell-established states in the D, D_s, B, and B_s families. The values located below the meson state represent the predicted mass and strong decay width in MeV units. Experimental evidence for some of the states shown in the figure may have been observed. For example, the $D_1^*(2760)$, $B_J(5840)$, and $B_J(5970)$ may be candidates of the $D(1^3D_1)$, $B(2^3S_1)$, $B(1D_2)$, respectively, while the $B_{sJ}(6109)$ and $B_{sJ}(6158)$ [or $B_{sJ}(6064)$ and $B_{sJ}(6114)$] may be candidates of the $1D$-wave states in the B_s family.

gives a narrow width. While for the $\mathcal{H}_I^{RC}$ of order $1/m^2$ given in Eq. (12), the second term containing $\boldsymbol{p}_j^2$, as the dominant term, contributes a sizeable value to the matrix element. This value is proportional to the square of the size parameter β^2 of the spatial wave function and comparable with that of $\sigma_j \cdot \boldsymbol{p}_j$ in magnitude. By constructive interference with the small contribution of $\mathcal{H}_I^{NR}$, the relativistic correction term $\mathcal{H}_I^{RC}$ of order $1/m^2$ leads to a large enhancement of the total widths. This mechanism also exists in the radially excited baryons [51,52].

V. PREDICTION

We have demonstrated that our model successfully describes the masses and widths of existing heavy-light mesons. To further examine our model, we also provide predictions for various masses and widths for heavy-light mesons. The numerical values have been given in Tables III and IV of the Appendix. Upon the confirmation of these states, our understanding of the structure of hadrons will be significantly enriched. Additionally, we provide the main decay channels and their branching ratios of these states in Fig. 3.

For the charmed meson sector, as shown in Fig. 1, the D_2' state in the D-meson family, and two states D_2 and D_2' in D_s family are not established in the experiments. These states exhibit narrow widths as illustrated in Fig. 2. In our model, we also provide the decay rates for these predicted states, as shown in Fig. 3. It should be emphasized that although the $D_1^*(2760)$ observed by the LHCb seems to favor the $D(1^3D_1)$ assignment, its existence should be further confirmed by other experiments. From the Fig. 3, one can see that the $D(^3D_1)$ dominantly decays into the $D_1(2420)\pi$ channel. It is most likely to be established in the three-body final state $D^*\pi\pi$ via the cascade decay $D(^3D_1) \to D_1(2420)\pi \to D^*\pi\pi$.

On the other hand, several excited states of B and B_s mesons remain unobserved, with notable examples being the 1^3P_0 and $1P_1$ states of B and B_s. Although the $B_J(5732)$ may favor the $B(1P_1)$ assignment, its spin-parity numbers and resonance parameters require to be further confirmed by future experiments. In our model, we predict the masses of $B(1^3P_0)$ and $B(1P_1)$ to be 5573 and 5656 MeV, respectively, which is consistent with those predicted in Refs. [87,90,91]. The $B(1^3P_0)$ and $B(1P_1)$ should be broad states with a width of $\Gamma \sim 300$ MeV, dominantly decaying into $B\pi$ and $B^*\pi$, respectively. Our predicted widths are comparable with results found in Ref. [92]. While in the B_s-meson family, the masses of $B_s(1^3P_0)$ and $B_s(1P_1)$ are predicted to be 5693 and 5767 MeV here, which are in good agreement with those from lattice QCD [93,94] and other coupled-channel models [75,76,95–99]. The predicted masses of the $B_s(1^3P_0)$ and $B_s(1P_1)$ states are lower than the BK and B^*K threshold, respectively. Thus, both $B_s(1^3P_0)$ and $B_s(1P_1)$ should be very narrow states which is similar as $D_{s0}^*(2317)$ and $D_{s1}(2460)$.

Additionally, numerous negative parity beauty mesons remain to be discovered in experimental searches. We would like to highlight a few notable cases. By comparing with the masses, we find that the $B_J(5840)$ favors the 2^3S_1 state, which is consistent with the assignment in Ref. [100]. The partial width ratio $\Gamma(B\pi)/\Gamma(B^*\pi) \simeq 0.55$ can be subject to verification in future experiments. The newly observed structures, $B_{sJ}(6064)$ and $B_{sJ}(6114)$, in the B^+K^- mass spectrum at LHCb [101], may potentially be explained by the presence of $B_s(1^3D_3)$ and $B_s(1^3D_1)$ states. Their primary predicted decay channel is B^+K^-. In addition, these two structures could also be caused by higher mass resonances $B_{sJ}(6109)$ and $B_{sJ}(6158)$, respectively, which mainly decay into $B^{*+}K^-$.

VI. SUMMARY

In this study, we propose a unified unquenched quark model framework, which successfully provides comprehensive mass spectra, decay widths, and strong decay branch widths for the D, D_s, B, and B_s sectors. This

unquenched quark model not only combines the traditional quark model and the coupled-channel effects based on chiral dynamics but also incorporates a relativistic correction term for describing the strong transition amplitude. These theoretical approaches and strategies adopted in the present work ensure that our model is excellent for simultaneously describing the masses and decay widths of all existing heavy-light mesons.

Notably, the low-mass nature of $D_{s0}^*(2317)$ and $D_{s1}(2460)$ can be reasonably understood in the unquenched quark model with chiral dynamics, moreover, the broad widths of the radial excitations $D_0(2550)/D_{s0}(2590)$ and $D_1^*(2600)/D_{s1}^*(2700)$ can be well described by including the relativistic correction term in the chiral interactions. Furthermore, our model predicts the masses, widths, and branching ratios of various new states, offering valuable guidance for their discovery in future experiments. Some of our predictions are consistent with the lattice data, strengthening our confidence in extending this model to the other hadron spectra, such as the light baryon spectrum and singly-heavy baryon spectrum. The success of the unquenched quark model presented in this work indicates it may be an important step for understanding the hadron spectrum.

ACKNOWLEDGMENTS

We thank useful discussions from Qiang Zhao, Xiang Liu, Zhi-Yong Zhou, and A. J. Arifi. This work is supported by the National Natural Science Foundation of China under Grants No. 12175065 and No. 12235018 (X. H. Z), No. 12175239 and No. 12221005 (J. J. W), and by the National Key R & D Program of China under Contract No. 2020YFA0406400 (J. J. W), and supported by Chinese Academy of Sciences under Grant No. YSBR-101 (J. J. W).

APPENDIX

1. Potential model

The bare mass and numerical wave functions of the heavy-light meson are calculate by a semirelativistic potential quark model. The effective Hamiltonian in the model is given by

$$\mathcal{H}_0 = \sqrt{\mathbf{p}_1^2 + m_1^2} + \sqrt{\mathbf{p}_2^2 + m_2^2} + V(r), \tag{A1}$$

where the first two terms stand for the kinetic energies for the light antiquark $\bar{q}$ and heavy quark Q, respectively, $V(r)$ stands for the effective potentials between two quarks, which is given by

$$V(r) = V_0(r) + V_{sd}(r). \tag{A2}$$

Here $V_0(r)$ is the well-known Cornell potential [102]

$$V_0(r) = -\frac{4}{3}\frac{\alpha_s(r)}{r} + br + C_0, \tag{A3}$$

which includes the color Coulomb interaction, linear confinement, and zero point energy C_0. The $V_{sd}(r)$ is the spin-dependent part, we adopted the widely used form [103,104]

$$V_{sd}(r) = \frac{32\pi\alpha_s(r)\cdot\sigma^3 e^{-\sigma^2 r^2}}{9\sqrt{\pi^3}\tilde{m}_1 m_2}\mathbf{S_1}\cdot\mathbf{S_2} + \frac{4}{3}\frac{\alpha_s(r)}{\tilde{m}_1 m_2}\frac{1}{r^3}\left(\frac{3\mathbf{S}_1\cdot\mathbf{r}\mathbf{S}_2\cdot\mathbf{r}}{r^2} - \mathbf{S}_1\cdot\mathbf{S}_2\right) + H_{LS}. \tag{A4}$$

In Eq. (A4), the first term is the spin-spin contact hyperfine potential, the second term is the tensor potential, the H_{LS} stands for the spin-orbit interaction, which can be decomposed into symmetric part $H_{\rm sym}$ and antisymmetric part $H_{\rm anti}$:

$$H_{\rm sym} = \frac{\mathbf{S}+\cdot\mathbf{L}}{2}\left[\left(\frac{1}{2\tilde{m}_1^2} + \frac{1}{2m_2^2}\right)\left(\frac{4\alpha_s(r)}{3r^3} - \frac{b}{r}\right) + \frac{8\alpha_s(r)}{3\tilde{m}_1 m_2 r^3}\right], \tag{A5}$$

$$H_{\rm anti} = \frac{\mathbf{S}_-\cdot\mathbf{L}}{2}\left(\frac{1}{2\tilde{m}_1^2} - \frac{1}{2m_2^2}\right)\left(\frac{4\alpha_s(r)}{3r^3} - \frac{b}{r}\right). \tag{A6}$$

In these equations, $\mathbf{L}$ is the relative orbital angular momentum of the $Q\bar{q}$ system; $\mathbf{S}_1$ and $\mathbf{S}_2$ are the spins of the light and heavy quarks, respectively, and $\mathbf{S}_\pm \equiv \mathbf{S}_1 \pm \mathbf{S}_2$. The antisymmetric part of the spin-orbit interaction, $H_{\rm anti}$, can cause a configuration mixing between spin-triplet n^3L_J and spin-singlet n^1L_J for the $Q\bar{q}$ system. Thus, the physical states nL_J and nL_J' are expressed as

$$\begin{pmatrix} nL_J \\ nL_J' \end{pmatrix} = \begin{pmatrix} \cos\theta_{nL} & \sin\theta_{nL} \\ -\sin\theta_{nL} & \cos\theta_{nL} \end{pmatrix}\begin{pmatrix} n^1L_J \\ n^3L_J \end{pmatrix}, \tag{A7}$$

where $J = L = 1, 2, 3\cdots$, and the θ_{nL} is the mixing angle. In this work, nL_J and nL_J' correspond to the lower-mass and higher-mass mixed states, respectively, as often adopted in the literature. This mixing angle can be perturbatively determined with the nondiagonal matrix element $\langle n^1L_J|H_{\rm anti}|n^3L_J\rangle$.

The running coupling constant $\alpha_s(r)$ adopted a parametrized form, $\alpha_s(r) = \sum_{i=1,2,3}\alpha_i\frac{2}{\sqrt{\pi}}\int_0^{\gamma_i r} e^{-x^2}dx$, in the coordinate space. In the different heavy-light meson systems, we set the consistent parameters $\alpha_2 = 0.15$, $\alpha_3 = 0.20$, $\gamma_1 = 1/2$, $\gamma_2 = \sqrt{10}/2$, and $\gamma_3 = \sqrt{1000}/2$, which are the same as those adopted in Refs. [12,14,103]. The parameter α_1 is slightly different for $D_{(s)}$ and $B_{(s)}$ spectra for a better description of the mass spectrum, as shown in the value in Table II. It should be mentioned that in the spin-dependent

TABLE II. Potential model parameters for quenched and unquenched mass spectra.

	$m_{c/b}$ (GeV)	$m_{u,d}$ (GeV)	$\tilde{m}_{u,d}$ (GeV)	m_s (GeV)	$\tilde{m}_s$ (GeV)	α_1	b (GeV^2)	σ (GeV)	C_0 (MeV)	r_c (fm)
Quenched										
D	1.45	0.45	0.64	⋯	⋯	0.28	0.180	0.953	−302.0	0.332
D_s	1.45	⋯	⋯	0.55	0.70	0.28	0.180	0.990	−267.0	0.320
B	4.80	0.45	0.64	⋯	⋯	0.22	0.180	0.870	−246.0	0.266
B_s	4.80	⋯	⋯	0.55	0.70	0.22	0.180	0.965	−218.0	0.253
Unquenched										
D	1.45	0.35	0.64	⋯	⋯	0.38	0.180	0.930	−179.0	0.341
D_s	1.45	⋯	⋯	0.55	0.70	0.38	0.180	0.882	−212.0	0.325
B	4.80	0.35	0.64	⋯	⋯	0.25	0.180	0.870	−172.0	0.270
B_s	4.80	⋯	⋯	0.55	0.70	0.25	0.180	0.939	−200.0	0.256

potentials, we have replaced the light quark mass m_1 with $\tilde{m}_1$ to include some relativistic corrections. By using the Gaussian expansion method [105] to solve the Schrödinger equation, the bare mass and numerical wave functions for heavy-light mesons are derived. Detailed discussions on the numerical calculation techniques involving Gaussian expansion can be found in our previous work [31].

2. Model parameters

In our unquenched calculations, there are 11 parameters $\{b, \alpha_1, \sigma, C_0, m_c, m_b, m_{u/d}, m_s, \tilde{m}_{u/d}, \tilde{m}_s, r_c\}$ in the potential model Hamiltonian $\mathcal{H}_0$, while there are five parameters $\{\delta, f_\pi, f_K, f_\eta, \mu_q\}$ in the effective interaction $\mathcal{H}_I$ described within the chiral quark model. Furthermore, there are four subtraction points M_0 for the $D_{(s)}$ and $B_{(s)}$ spectra, and one cutoff parameter Λ in the suppressed factor.

The parameter set $\{b, \alpha_1, \sigma, C_0, m_c, m_b, m_{u/d}, m_s, \tilde{m}_{u/d}, \tilde{m}_s, r_c\}$ of the potential model Hamiltonian $\mathcal{H}_0$ have been listed in Table II. The slope parameter b for the linear potential is fixed with $b = 0.18$ GeV^2, which is a typical value adopted in various relativistic potential models [11,15,103,106]. For the D-meson spectrum, the parameter set $\{\alpha_1, \sigma, C_0, m_{u/d}, m_c, \tilde{m}_{u/d}\}$ is determined by the six well-established states: $D(1865)^0$, $D^*(2007)^0$, $D_1(2420)^0$, $D_1(2430)^0$, $D_2^*(2460)^0$, and $D_3^*(2750)$. The m_c, $m_{u/d}$, α_1, and C_0 are mainly constrained by the overall behavior of the mass spectrum of the $D(1S)$, $D(1P)$, and $D(1D)$ states. While the parameters $\tilde{m}_{u/d}$ and σ appearing in the spin-dependent potentials are determined by fitting the mass splittings $M[D_2^*(2460) - D_1(2420)]_{\text{exp}} \simeq 34$ MeV and $M[D^*(2007) - D(1865)]_{\text{exp}} \simeq 145$ MeV. For the D_s-meson sector, the parameters m_c and α_1 are taken the same values as those determined by the D-meson spectrum. The other four parameters $\{\sigma, C_0, m_s, \tilde{m}_s\}$ are determined by the four well-established states: $D_s(1969)$, $D_s^*(2112)$, $D_{s1}(2536)$, and $D_{s2}^*(2573)$. The C_0 and m_s can be easily constrained by the overall behavior of the mass spectrum of these well-established $1S$ and $1P$ states. While the other two parameters $\tilde{m}_s$ and σ can be well constrained by the mass splittings $M[D_{s2}^*(2573) - D_{s1}(2536)]_{\text{exp}} \simeq 31$ MeV and $M[D_s^*(2112) - D_s(1969)]_{\text{exp}} \simeq 143$ MeV.

For the B- and B_s-meson sectors, the light quark masses $m_{u/d}$, m_s, $\tilde{m}_{u/d}$, and $\tilde{m}_s$ are taken the same values as those determined by the D- and D_s-meson spectra for consistency. The other four parameters $\{\alpha_1, \sigma, C_0, m_b\}$ for the B-meson are determined by the four well-established states: $B(5280)$, $B^*(5325)$, $B_1(5721)$, and $B_2^*(5747)$. The three parameters α_1, C_0, and m_b are mainly constrained by the overall behavior of the mass spectrum of these well-established $1S$ and $1P$ states. Meanwhile, the parameter σ is determined by fitting the mass splitting $M[B^*(5325) - B(5280)]_{\text{exp}} \simeq 45$ MeV. For the B_s-meson sector, the two parameters m_b and α_1 are taken the same values determined by the B-meson spectrum for consistency. Finally, the two parameters $\{\sigma, C_0\}$ for the B_s meson can be easily determined by fitting the masses of the well-established states $B_s(5367)$ and $B_s^*(5416)$.

It should be mentioned that we cannot obtain stable solutions for some states due to the singular behavior of $1/r^3$ in the spin-orbit and tensor potentials. To overcome the singular behavior, following the method of our previous works [107,108], we introduce a cutoff distance r_c in the calculation. Within a small range $r \in (0, r_c)$, we let $1/r^3 = 1/r_c^3$. It is found that the mass of the 1^3P_0 state is more sensitive to the cutoff distance r_c due to its relatively larger factor $\langle \mathbf{S}_+ \cdot \mathbf{L} \rangle$ than the other excited meson states. Thus, the cutoff parameters r_c for the $D_{(s)}$- and $B_{(s)}$-meson spectra are determined by fitting the masses of $D_{(s)}(1^3P_0)$ and $B_{(s)}(1^3P_0)$ obtained with the method of perturbation [32,109,110]. In this method, the singular $1/r^3$ terms in the spin-orbit and tensor potentials are treated as perturbative terms. First, by neglecting the contributions of these singular terms we obtain the zero-order mass m and spatial wave function, then by using the wave function we further calculate the mass correction term δm from the perturbative terms, finally, we obtained the full mass $M = m + \delta m$ for fitting. With the perturbation method one can obtain a fairly accurate mass, although

one cannot include the effects of the spin-dependent interactions on the wave functions. By introducing the cutoff distance r_c, we can nonperturbatively include the corrections from spin-orbit and tensor potentials to both the mass and wave function.

There are five parameters $\{\delta,\ f_\pi,\ f_K,\ f_\eta,\ \mu\}$ in the effective chiral interaction $\mathcal{H}_I$. The dimensionless parameter δ accounting for the strength of quark-meson couplings is fixed with $\delta = 0.557$. It has been determined in a previous work of our group by fitting the decay width of the $\Sigma_c(2520)$ baryon [58]. Research shows that this fitted value has general applicability and can be successfully applied to study the similar strong decay processes of the heavy hadron resonances [27–31,58–60]. The decay constants f_π, f_K and f_η for π, K and η are taken as $f_\pi = 132$ MeV, and $f_K = f_\eta = 160$ MeV. For the calculation of the strong transition amplitude $\langle BC, \boldsymbol{q}|\mathcal{H}_I|A\rangle$ within the chiral quark model, one can find that the relativistic correction term $\mathcal{H}_I^{RC}$ is sensitive to the effective mass of the light u/d quarks due to the factor $1/\mu^2 = (1/m_j + 1/m'_j)^2$. It is found that the $\mathcal{H}_I^{RC}$ term plays a dominant role in the strong decay of the radially excited states. To obtain a good description of the strong decay properties for the radially excited heavy-light meson states, we take $\mu_q = 225$ MeV, which corresponds to the effective mass of the u/d quark $m_{u/d} = 450$ MeV, which is slightly larger than that used in the potential model for calculating the bare masses of heavy-light mesons. The operator $\mathcal{H}_I$ is derived from the effective Lagrangians with a weak binding approximation, the interaction between the quarks is not seriously considered as that in the potential model. Thus, the effective u/d quark mass in the chiral quark model should be slightly different from that in the potential model.

In the unquenched picture, we have adopted the once-subtracted method as suggested in Ref. [45]. There is a subtraction point parameter M_0 for each mass spectrum. According to the method adopted in the literature [39,45,46], the subtraction point M_0 is adopted the ground masses, 1865, 1969, 5280, and 5367 MeV for the D-, D_s-, B-, and B_s-meson families, respectively. In this case, the coupled-channel effects of the virtual channels on these ground states are entirely subtracted. Thus, the mass shifts $\Delta M(M, M_0)$ for the ground states $D_{(s)}/B_{(s)}(1^1S_0)$ are zero. The strong transition amplitude $\langle BC, \boldsymbol{q}|\mathcal{H}_I|A\rangle$ is crucial for our evaluation of the coupled-channel effects on the bare states and the strong decay widths.

The cutoff parameter Λ determines the scale at which chiral symmetry is broken. The typical range of Λ is about 0.8 ± 0.2 GeV. In the present work, we take $\Lambda = 0.78$ GeV for a better description of the masses of $D_{s0}^*(2317)$ and $D_{s1}(2460)$ by including coupled-channel effects.

3. More details of numerical results

The masses for the heavy-light meson states obtained from the quenched and unquenched quark models are listed in Table I. The decay widths of the heavy-light meson from the two methods are also listed in Table I. In method I, the decay widths are described without relativistic correction term $\mathcal{H}_I^{RC}$ by combining the spectrum from the unquenched quark model. In method II, the decay widths are described with relativistic correction term $\mathcal{H}_I^{RC}$ by combining the spectrum also from the unquenched quark model. It is found that with relativistic correction of the descriptions of the decay widths for the heavy-light states have an overall improvement.

In Tables III and IV, the mass shifts, and partial widths of the heavy-light meson states contributed by each channel are given. From the tables, one can find which channels play a crucial role in the mass shift of a heavy-light meson, and which channels dominate their strong decays. One also can see the details of the relativistic corrections to the partial widths of each channel. The partial width ratios between different decay channels and their branching fractions for each state can be obtained from these tables.

TABLE III. The mass shifts ΔM and partial widths (in MeV) of the D and D_s states. The bare masses obtained from the potential model are listed in square brackets. The strong decay widths, which combine the unquenched spectra and are described by nonrelativistic chiral interactions $\mathcal{H}_I^{NR}$, are further augmented by a relativistic correction term $\mathcal{H}_I^{RC}$. These widths are denoted as Γ_i^{NR} and Γ_i^{NR+RC}, respectively. The forbidden decay channel is denoted by "$\cdots$". The experimental data are taken from the PDG [6].

	$D(2^1S_0)$			$D(2^3S_1)$				$D(1^3P_0)$			$D(1^3P_2)$		
	ΔM	*as* $D_0(2550)$		ΔM	*as* $D_1^*(2600)$			ΔM	*as* $D_0^*(2300)$		ΔM	*as* $D_2^*(2460)$	
Channel	[2575]	Γ_i^{NR}	Γ_i^{NR+RC}	[2667]	Γ_i^{NR}	Γ_i^{NR+RC}	Channel	[2304]	Γ_i^{NR}	Γ_i^{NR+RC}	[2510]	Γ_i^{NR}	Γ_i^{NR+RC}
$D\pi$	$\cdots$	$\cdots$	$\cdots$	3.2	31.4	22.8	$D\pi$	−114.6	153.7	284.2	−16.9	26.9	21.8
$D^*\pi$	−35.8	24.8	218.2	−2.1	1.8	82.1	$D^*\pi$	$\cdots$	$\cdots$	$\cdots$	−23.7	18.2	12.6
$D\eta$	$\cdots$	$\cdots$	$\cdots$	−0.5	0.9	2.7	$D\eta$	$\cdots$	$\cdots$	$\cdots$	−1.8	0.1	0.1
$D^*\eta$	$\cdots$	$\cdots$	$\cdots$	−1.9	0.2	3.1	*Total*	**−114.6**	**153.7**	**284.2**	**−42.4**	**45.2**	**34.5**
D_sK	$\cdots$	$\cdots$	$\cdots$	−1.4	1.8	3.8	*Exp.*	$\cdots$	**229 ± 16**		$\cdots$	**47.3 ± 0.8**	
D_s^*K	$\cdots$	$\cdots$	$\cdots$	−2.8	0.03	1.0							

(Table continued)

TABLE III. *(Continued)*

	$D(2^1S_0)$			$D(2^3S_1)$				$D(1^3P_0)$			$D(1^3P_2)$		
	ΔM	*as* $D_0(2550)$		ΔM	*as* $D_1^*(2600)$			ΔM	*as* $D_0^*(2300)$		ΔM	*as* $D_2^*(2460)$	
Channel	[2575]	Γ_i^{NR}	Γ_i^{NR+RC}	[2667]	Γ_i^{NR}	Γ_i^{NR+RC}	Channel	[2304]	Γ_i^{NR}	Γ_i^{NR+RC}	[2510]	Γ_i^{NR}	Γ_i^{NR+RC}
$D_0^*(2300)\pi$	−36.5	13.0	14.3	⋯	⋯	⋯		$D(1P_1)$			$D(1P_1')$		
$D_1(2430)\pi$	⋯	⋯	⋯	−43.5	14.0	18.9		ΔM	*as*$D_1(2430)$		ΔM	*as*$D_1(2420)$	
$D_1(2420)\pi$	⋯	⋯	⋯	−6.8	0.2	0.02	Channel	[2449]	Γ_i^{NR}	Γ_i^{NR+RC}	[2471]	Γ_i^{NR}	Γ_i^{NR+RC}
$D_2^*(2460)\pi$	⋯	⋯	⋯	−10.4	0.02	0.01	$D^*\pi$	−57.4	120.1	309.0	−35.1	19.2	10.7
Total	**−72.3**	**37.8**	**232.5**	**−66.2**	**50.4**	**134.4**	*Total*	**−57.4**	**120.1**	**309.0**	**−35.1**	**19.2**	**10.7**
Exp.	⋯	**165 ± 24**		⋯	**141 ± 23**		*Exp.*	⋯	**314 ± 29**		⋯	**31.3 ± 1.9**	

	$D(1^3D_1)$			$D(1^3D_3)$				$D(1D_2)$			$D(1D_2')$		
	ΔM	*as* $D_1^*(2760)$		ΔM	*as* $D_3^*(2750)$			ΔM	*as* $D_2(2740)$		ΔM	$M = 2789$	
Channel	[2765]	Γ_i^{NR}	Γ_i^{NR+RC}	[2830]	Γ_i^{NR}	Γ_i^{NR+RC}	Channel	[2799]	Γ_i^{NR}	Γ_i^{NR+RC}	[2856]	Γ_i^{NR}	Γ_i^{NR+RC}
$D\pi$	−3.5	26.6	6.6	−5.6	12.2	13.8	$D^*\pi$	−5.1	22.7	23.2	−18.3	30.1	27.2
$D^*\pi$	−2.2	9.6	2.8	−10.0	14.3	14.4	$D^*\eta$	−0.9	5.0	1.8	−2.2	1.1	0.9
$D\eta$	−0.5	4.7	0.4	−0.8	0.8	0.8	D_s^*K	−1.9	8.6	2.3	−4.9	1.3	0.9
$D^*\eta$	−0.3	0.9	0.1	−1.2	0.3	0.4	$D_0^*(2300)\pi$	−2.2	0.02	1.2	−16.4	10.5	12.7
D_sK	−1.2	9.0	0.4	−1.6	0.9	1.0	$D_1(2430)\pi$	−4.2	0.4	0.5	−0.3	2.9	2E-3
D_s^*K	−0.6	0.6	0.04	−2.3	0.2	0.3	$D_1(2420)\pi$	−5.2	0.7	0.5	−10.6	8.9	0.9
$D_1(2430)\pi$	−8.3	0.03	0.2	−4.3	5.6	0.9	$D_2^*(2460)\pi$	−56.5	66.3	129.2	−14.5	3.8	6.5
$D_1(2420)\pi$	−88.3	64.0	92.8	−11.1	1.1	0.5	*Total*	**−76.0**	**103.7**	**158.7**	**−67.2**	**58.6**	**49.1**
$D_2^*(2460)\pi$	−11.9	0.02	0.01	−17.4	3.7	1.3	*Exp.*	⋯	**88 ± 19**		⋯	⋯	
Total	**−116.8**	**115.5**	**103.3**	**−54.3**	**39.1**	**33.4**							
Exp.	⋯	**177 ± 40**		⋯	**66 ± 5**								

	$D_s(2^1S_0)$			$D_s(2^3S_1)$				$D_s(1^3P_0)$			$D_s(1^3P_2)$		
	ΔM	*as* $D_{s0}(2590)$		ΔM	*as* $D_{s1}^*(2700)$			ΔM	*as* $D_{s0}^*(2317)$		ΔM	*as* $D_{s2}^*(2573)$	
Channel	[2677]	Γ_i^{NR}	Γ_i^{NR+RC}	[2753]	Γ_i^{NR}	Γ_i^{NR+RC}	Channel	[2372]	Γ_i^{NR}	Γ_i^{NR+RC}	[2597]	Γ_i^{NR}	Γ_i^{NR+RC}
DK	⋯	⋯	⋯	0.8	15.5	20.0	DK	−78.4	⋯	⋯	−15.2	15.9	11.7
D^*K	−43.7	11.0	65.7	−6.9	0.4	63.7	D^*K	⋯	⋯	⋯	−19.4	2.3	1.6
$D_s\eta$	⋯	⋯	⋯	−0.7	0.6	5.4	$D_s\eta$	⋯	⋯	⋯	−2.1	0.2	0.1
$D_s^*\eta$	⋯	⋯	⋯	−3.6	0.1	3.4	*Total*	**−78.4**	⋯		**−36.7**	**18.4**	**13.4**
Total	**−43.7**	**11.0**	**65.7**	**−10.4**	**16.6**	**92.5**	*Exp.*	⋯	**< 3.8**		⋯	**16.9 ± 0.7**	
Exp.	⋯	**89 ± 20**		⋯	**122 ± 10**								

	$D_s(1P_1)$			$D_s(1P_1)$		
	ΔM	*as* $D_{s1}(2460)$		ΔM	*as* $D_{s1}(2536)$	
Channel	[2533]	Γ_i^{NR}	Γ_i^{NR+RC}	[2546]	Γ_i^{NR}	Γ_i^{NR+RC}
D^*K	−57.8	⋯	⋯	−27.4	0.6	0.3
Total	**−57.8**	⋯		**−27.4**	**0.6**	**0.3**
Exp.	⋯	**< 3.5**		⋯	**0.92 ± 0.05**	

	$D_s(1^3D_1)$			$D_s(1^3D_3)$				$D_s(1D_2)$			$D_s(1D_2')$		
	ΔM	*as* $D_{s1}^*(2860)$		ΔM	*as* $D_{s3}^*(2860)$			ΔM	$M = 2870$		ΔM	$M = 2893$	
Channel	[2829]	Γ_i^{NR}	Γ_i^{NR+RC}	[2909]	Γ_i^{NR}	Γ_i^{NR+RC}	Channel	[2877]	Γ_i^{NR}	Γ_i^{NR+RC}	[2923]	Γ_i^{NR}	Γ_i^{NR+RC}
DK	−2.6	22.4	12.6	−5.2	13.3	10.8	D^*K	−3.4	23.1	22.4	−16.3	21.6	17.5
D^*K	−1.6	9.6	5.8	−9.2	12.3	10.0	$D_s^*\eta$	−1.5	6.3	2.6	−2.5	1.3	1.0
$D_s\eta$	−1.0	7.3	1.5	−0.8	1.1	0.9	$D_0^*(2300)K$	−1.8	2E-6	4E-3	−11.5	1.0	0.9
$D_s^*\eta$	−0.5	2.4	0.6	−1.2	0.5	0.1	*Total*	**−6.7**	**29.4**	**25.0**	**−30.3**	**23.9**	**19.4**
Total	**−5.7**	**41.7**	**20.5**	**−16.4**	**27.2**	**21.8**	*Exp.*	⋯	⋯		⋯	⋯	
Exp.	⋯	**159 ± 80**		⋯	**53 ± 10**								

TABLE IV. The mass shifts ΔM and partial widths (in MeV) of the B and B_s states. The bare masses obtained from the potential model are listed in square brackets. The strong decay widths, which combine the unquenched spectra and are described by nonrelativistic chiral interactions $\mathcal{H}_I^{NR}$, are further augmented by a relativistic correction term $\mathcal{H}_I^{RC}$. These widths are denoted as Γ_i^{NR} and Γ_i^{NR+RC}, respectively. The forbidden decay channel is denoted by "$\cdots$". The experimental data are taken from the PDG [6].

	$B(2^1S_0)$			$B(2^3S_1)$				$B(1^3P_0)$			$B(1^3P_2)$		
	ΔM	$M=5781$		ΔM	$as\,B_J(5840)^+$			ΔM	$M=5573$		ΔM	$as\,B_2^*(5747)^{+/0}$	
Channel	[5882]	Γ_i^{NR}	Γ_i^{NR+RC}	[5908]	Γ_i^{NR}	Γ_i^{NR+RC}	Channel	[5704]	Γ_i^{NR}	Γ_i^{NR+RC}	[5780]	Γ_i^{NR}	Γ_i^{NR+RC}
$B\pi$	$\cdots$	$\cdots$	$\cdots$	-3.3	2.8	96.3	$B\pi$	-131.2	153.4	282.5	-18.4	17.1/17.6	11.7/12.0
$B^*\pi$	-37.8	3.8	252.1	-14.5	0.1	175.4	$B^*\pi$	$\cdots$	$\cdots$	$\cdots$	-25.3	16.9/17.4	10.7/11.0
$B\eta$	$\cdots$	$\cdots$	$\cdots$	-1.2	0.02	0.8	*Total*	**-131.2**	**153.4**	**282.5**	**-43.7**	**34.0/35.0**	**22.4/23.0**
$B^*\eta$	$\cdots$	$\cdots$	$\cdots$	-1.9	$\cdots$	$\cdots$	*Exp.*	$\cdots$	$\cdots$		$\cdots$	**$20\pm5/24.2\pm1.7$**	
B_sK	$\cdots$	$\cdots$	$\cdots$	-2.0	$\cdots$	$\cdots$							
B_s^*K	$\cdots$	$\cdots$	$\cdots$	-3.4	$\cdots$	$\cdots$							
$B(1^3P_0)\pi$	-63.4	31.2	37.2	$\cdots$	$\cdots$	$\cdots$		$B(1P_1)$			$B(1P_1')$		
$B(1P_1)\pi$	$\cdots$	$\cdots$	$\cdots$	-50.0	16.4	23.2		ΔM	$as\,B_J^*(5732)$		ΔM	$as\,B_1(5721)^{+/0}$	
$B_1(5721)\pi$	$\cdots$	$\cdots$	$\cdots$	-6.0	$\cdots$	$\cdots$	Channel	[5757]	Γ_i^{NR}	Γ_i^{NR+RC}	[5771]	Γ_i^{NR}	Γ_i^{NR+RC}
$B_2^*(5747)\pi$	$\cdots$	$\cdots$	$\cdots$	-9.8	$\cdots$	$\cdots$	$B^*\pi$	-101.1	149.2	314.7	-40.4	24.6/24.6	13.3/13.3
Total	**-101.2**	**35.0**	**289.3**	**-92.1**	**19.3**	**295.7**	*Total*	**-101.1**	**149.2**	**314.7**	**-40.4**	**24.6/24.6**	**13.3/13.3**
Exp.	$\cdots$	$\cdots$		$\cdots$	**224 ± 104**		*Exp.*	$\cdots$	**128 ± 18**		$\cdots$	**$31\pm6/27.5\pm3.4$**	

	$B(1^3D_1)$			$B(1^3D_3)$				$B(1D_2)$			$B(1D_2')$		
	ΔM	$M=5949$		ΔM	$M=6009$			ΔM	$M=5953$		ΔM	$M=6051$	
Channel	[6095]	Γ_i^{NR}	Γ_i^{NR+RC}	[6070]	Γ_i^{NR}	Γ_i^{NR+RC}	Channel	[6055]	Γ_i^{NR}	Γ_i^{NR+RC}	[6129]	Γ_i^{NR}	Γ_i^{NR+RC}
$B\pi$	-6.2	35.1	13.4	-9.5	15.2	15.9	$B^*\pi$	-8.4	38.8	21.1	-25.1	42.1	40.7
$B^*\pi$	-3.2	15.7	6.2	-13.0	17.6	17.2	$B^*\eta$	-1.0	3.7	0.4	-2.9	1.1	0.8
$B\eta$	-0.7	4.5	0.3	-1.1	0.3	0.3	B_s^*K	-2.0	3.3	0.2	-6.2	1.3	0.8
$B^*\eta$	-0.3	1.3	0.1	-1.4	0.2	0.2	$B(1^3P_0)\pi$	-3.2	6E-5	0.5	-16.2	22.4	29.0
B_sK	-1.6	6.4	0.1	-2.0	0.3	0.2	$B(1P_1)\pi$	-4.1	0.3	0.6	-0.7	6.0	0.5
B_s^*K	-0.8	1.0	0.02	-2.7	0.1	0.1	$B_1(5721)\pi$	-4.7	0.08	0.1	-9.2	6.7	0.1
$B(1P_1)\pi$	-12.2	0.2	3.3	-2.4	10.5	0.6	$B_2^*(5747)\pi$	-79.0	50.6	75.6	-18.0	4.7	8.9
$B_1(5721)\pi$	-104.8	78.6	117.7	-13.0	0.5	0.1	*Total*	**-102.4**	**96.8**	**98.5**	**-78.3**	**84.3**	**80.8**
$B_2^*(5747)\pi$	-16.5	0.1	0.03	-15.7	2.1	0.3							
Total	**-146.3**	**142.9**	**141.2**	**-60.8**	**46.8**	**34.9**							

	$B_s(2^1S_0)$			$B_s(2^3S_1)$				$B_s(1^3P_0)$			$B_s(1^3P_2)$		
	ΔM	$M=5919$		ΔM	$M=5957$			ΔM	$M=5693$		ΔM	$asB_{s2}^*(5840)^0$	
Channel	[5969]	Γ_i^{NR}	Γ_i^{NR+RC}	[5996]	Γ_i^{NR}	Γ_i^{NR+RC}	Channel	[5772]	Γ_i^{NR}	Γ_i^{NR+RC}	[5864]	Γ_i^{NR}	Γ_i^{NR+RC}
BK	$\cdots$	$\cdots$	$\cdots$	-8.1	0.4	61.2	BK	-78.9	$\cdots$	$\cdots$	-14.3	1.99	1.44
B^*K	-49.7	16.1	125.0	-23.0	5.9	98.1	B^*K	$\cdots$	$\cdots$	$\cdots$	-19.1	0.19	0.13
$B_s\eta$	$\cdots$	$\cdots$	$\cdots$	-3.4	0.05	3.1	*Total*	**-78.9**	$\cdots$		**-33.4**	**2.18**	**1.57**
$B_s^*\eta$	$\cdots$	$\cdots$	$\cdots$	-4.7	$\cdots$	$\cdots$	*Exp.*	$\cdots$	$\cdots$		$\cdots$	**1.49 ± 0.27**	
Total	**-49.7**	**16.1**	**125.0**	**-39.2**	**6.4**	**162.4**		$B_s(1P_1)$			$B_s(1P_1')$		
Exp.	$\cdots$	$\cdots$		$\cdots$	$\cdots$			ΔM	$M=5767$		ΔM	$asB_{s1}(5830)^0$	
							Channel	[5840]	Γ_i^{NR}	Γ_i^{NR+RC}	[5842]	Γ_i^{NR}	Γ_i^{NR+RC}
							B^*K	-72.8	$\cdots$	$\cdots$	-29.4	0.05	0.03
							Total	**-72.8**	$\cdots$		**-29.4**	**0.05**	**0.03**
							Exp.	$\cdots$	$\cdots$		$\cdots$	**0.5 ± 0.4**	

(Table continued)

TABLE IV *(Continued)*

	$B_s(1^3D_1)$			$B_s(1^3D_3)$				$B_s(1D_2)$			$B_s(1D_2')$		
	ΔM	$M=6146$		ΔM	$M=6122$			ΔM	$as\,B_{sJ}(6109)$		ΔM	$asB_{sJ}(6158)$	
Channel	[6156]	Γ_i^{NR}	Γ_i^{NR+RC}	[6146]	Γ_i^{NR}	Γ_i^{NR+RC}	Channel	[6131]	Γ_i^{NR}	Γ_i^{NR+RC}	[6191]	Γ_i^{NR}	Γ_i^{NR+RC}
BK	−4.8	43.5	24.4	−9.1	12.0	12.5	B^*K	−6.3	52.5	28.5	−24.0	31.7	30.4
B^*K	−2.5	20.9	11.8	−12.3	12.4	12.3	$B_s^*\eta$	−2.2	10.5	2.2	−3.6	1.7	1.2
$B_s\eta$	−1.5	12.8	2.4	−1.2	0.4	0.4	*Total*	**−8.5**	**63.0**	**30.7**	**−27.6**	**33.4**	**31.6**
$B_s^*\eta$	−0.7	5.2	1.0	−1.6	0.3	0.3	*Exp.*	⋯	**22 ± 9**		⋯	**72 ± 43**	
Total	**−9.5**	**82.4**	**39.6**	**−24.2**	**25.1**	**25.5**							

[1] M. Gell-Mann, A schematic model of baryons and mesons, Phys. Lett. **8**, 214 (1964).
[2] G. Zweig, An SU(3) model for strong interaction symmetry and its breaking. Version 1, CERN-TH-401.
[3] G. Zweig, An SU(3) model for strong interaction symmetry and its breaking. Version 2, CERN-TH-412.
[4] S. K. Choi *et al.* (Belle Collaboration), Observation of a narrow charmonium-like state in exclusive $B^{\pm}\to K^{\pm}\pi^{+}\pi^{-}J/\psi$ decays, Phys. Rev. Lett. **91**, 262001 (2003).
[5] B. Aubert *et al.* (*BABAR* Collaboration), Observation of a narrow meson decaying to $D_s^{+}\pi^{0}$ at a mass of 2.32-GeV/c^2, Phys. Rev. Lett. **90**, 242001 (2003).
[6] R. L. Workman *et al.* (Particle Data Group), Review of Particle Physics, Prog. Theor. Exp. Phys. **2022**, 083C01 (2022).
[7] H. X. Chen, W. Chen, X. Liu, Y. R. Liu, and S. L. Zhu, A review of the open charm and open bottom systems, Rep. Prog. Phys. **80**, 076201 (2017).
[8] H. X. Chen, W. Chen, X. Liu, Y. R. Liu, and S. L. Zhu, An updated review of the new hadron states, Rep. Prog. Phys. **86**, 026201 (2023).
[9] S. Theberge, A. W. Thomas, and G. A. Miller, The cloudy bag model. 1. The (3,3) resonance, Phys. Rev. D **22**, 2838 (1980); **23**, 2106(E) (1981).
[10] J. Vijande, F. Fernandez, and A. Valcarce, Constituent quark model study of the meson spectra, J. Phys. G **31**, 481 (2005).
[11] D. Ebert, R. N. Faustov, and V. O. Galkin, Heavy-light meson spectroscopy and Regge trajectories in the relativistic quark model, Eur. Phys. J. C **66**, 197 (2010).
[12] J. B. Liu and M. Z. Yang, Spectrum of the charmed and b-flavored mesons in the relativistic potential model, J. High Energy Phys. 07 (2014) 106.
[13] J. B. Liu and C. D. Lu, Spectra of heavy-light mesons in a relativistic model, Eur. Phys. J. C **77**, 312 (2017).
[14] J. B. Liu and M. Z. Yang, Spectrum of higher excitations of B and D mesons in the relativistic potential model, Phys. Rev. D **91**, 094004 (2015).
[15] D. Ebert, V. O. Galkin, and R. N. Faustov, Mass spectrum of orbitally and radially excited heavy-light mesons in the relativistic quark model, Phys. Rev. D **57**, 5663 (1998); **59**, 019902(E) (1999).
[16] S. Godfrey and K. Moats, Properties of excited charm and charm-strange mesons, Phys. Rev. D **93**, 034035 (2016).
[17] S. Godfrey, K. Moats, and E. S. Swanson, B and B_s meson spectroscopy, Phys. Rev. D **94**, 054025 (2016).
[18] I. Asghar, B. Masud, E. S. Swanson, F. Akram, and M. Atif Sultan, Decays and spectrum of bottom and bottom strange mesons, Eur. Phys. J. A **54**, 127 (2018).
[19] D. M. Li, P. F. Ji, and B. Ma, The newly observed open-charm states in quark model, Eur. Phys. J. C **71**, 1582 (2011).
[20] Q. F. Lü, T. T. Pan, Y. Y. Wang, E. Wang, and D. M. Li, Excited bottom and bottom-strange mesons in the quark model, Phys. Rev. D **94**, 074012 (2016).
[21] P. Colangelo, F. De Fazio, F. Giannuzzi, and S. Nicotri, New meson spectroscopy with open charm and beauty, Phys. Rev. D **86**, 054024 (2012).
[22] Y. Sun, Q. T. Song, D. Y. Chen, X. Liu, and S. L. Zhu, Higher bottom and bottom-strange mesons, Phys. Rev. D **89**, 054026 (2014).
[23] Q. T. Song, D. Y. Chen, X. Liu, and T. Matsuki, Higher radial and orbital excitations in the charmed meson family, Phys. Rev. D **92**, 074011 (2015).
[24] Q. T. Song, D. Y. Chen, X. Liu, and T. Matsuki, Charmed-strange mesons revisited: Mass spectra and strong decays, Phys. Rev. D **91**, 054031 (2015).
[25] J. Ferretti and E. Santopinto, Open-flavor strong decays of open-charm and open-bottom mesons in the $^3P_0$ model, Phys. Rev. D **97**, 114020 (2018).
[26] M. Di Pierro and E. Eichten, Excited heavy-light systems and hadronic transitions, Phys. Rev. D **64**, 114004 (2001).
[27] X. H. Zhong and Q. Zhao, Strong decays of heavy-light mesons in a chiral quark model, Phys. Rev. D **78**, 014029 (2008).
[28] X. H. Zhong and Q. Zhao, Strong decays of newly observed D_{sJ} states in a constituent quark model with effective Lagrangians, Phys. Rev. D **81**, 014031 (2010).

[29] X. H. Zhong, Strong decays of the newly observed $D(2550)$, $D(2600)$, $D(2750)$, and $D(2760)$, Phys. Rev. D **82**, 114014 (2010).
[30] L. Y. Xiao and X. H. Zhong, Strong decays of higher excited heavy-light mesons in a chiral quark model, Phys. Rev. D **90**, 074029 (2014).
[31] R. H. Ni, Q. Li, and X. H. Zhong, Mass spectra and strong decays of charmed and charmed-strange mesons, Phys. Rev. D **105**, 056006 (2022).
[32] Q. li, R. H. Ni, and X. H. Zhong, Towards establishing an abundant B and B_s spectrum up to the second orbital excitations, Phys. Rev. D **103**, 116010 (2021).
[33] D. S. Hwang and D. W. Kim, Mass of $D_{sJ}^*(2317)$ and coupled channel effect, Phys. Lett. B **601**, 137 (2004).
[34] Y. B. Dai, C. S. Huang, C. Liu, and S. L. Zhu, Understanding the $D_{sJ}^+(2317)$ and $D_{sJ}^+(2460)$ with sum rules in HQET, Phys. Rev. D **68**, 114011 (2003).
[35] Z. Y. Zhou and Z. Xiao, Two-pole structures in a relativistic Friedrichs–Lee-QPC scheme, Eur. Phys. J. C **81**, 551 (2021).
[36] X. G. Wu and Q. Zhao, The mixing of $D_{s1}(2460)$ and $D_{s1}(2536)$, Phys. Rev. D **85**, 034040 (2012).
[37] D. Mohler, C. B. Lang, L. Leskovec, S. Prelovsek, and R. M. Woloshyn, $D_{s0}^*(2317)$ meson and D-meson-kaon scattering from lattice QCD, Phys. Rev. Lett. **111**, 222001 (2013).
[38] C. B. Lang, L. Leskovec, D. Mohler, S. Prelovsek, and R. M. Woloshyn, Ds mesons with DK and D^*K scattering near threshold, Phys. Rev. D **90**, 034510 (2014).
[39] Z. Y. Zhou and Z. Xiao, Hadron loops effect on mass shifts of the charmed and charmed-strange spectra, Phys. Rev. D **84**, 034023 (2011).
[40] J. M. Xie, M. Z. Liu, and L. S. Geng, $D_{s0}(2590)$ as a dominant $c\bar{s}$ state with a small D^*K component, Phys. Rev. D **104**, 094051 (2021).
[41] W. Hao, Y. Lu, and B. S. Zou, Coupled channel effects for the charmed-strange mesons, Phys. Rev. D **106**, 074014 (2022).
[42] Y. S. Kalashnikova, Coupled-channel model for charmonium levels and an option for $X(3872)$, Phys. Rev. D **72**, 034010 (2005).
[43] T. Barnes and E. S. Swanson, Hadron loops: General theorems and application to charmonium, Phys. Rev. C **77**, 055206 (2008).
[44] Y. Lu, M. N. Anwar, and B. S. Zou, Coupled-channel effects for the bottomonium with realistic wave functions, Phys. Rev. D **94**, 034021 (2016).
[45] M. R. Pennington and D. J. Wilson, Decay channels and charmonium mass-shifts, Phys. Rev. D **76**, 077502 (2007).
[46] M. X. Duan and X. Liu, Where are 3P and higher P-wave states in the charmonium family?, Phys. Rev. D **104**, 074010 (2021).
[47] A. Manohar and H. Georgi, Chiral quarks and the nonrelativistic quark model, Nucl. Phys. **B234**, 189 (1984).
[48] Z. P. Li, The threshold pion photoproduction of nucleons in the chiral quark model, Phys. Rev. D **50**, 5639 (1994).
[49] Z. P. Li, H. X. Ye, and M. H. Lu, An unified approach to pseudoscalar meson photoproductions off nucleons in the quark model, Phys. Rev. C **56**, 1099 (1997).
[50] Q. Zhao, J. S. Al-Khalili, Z. P. Li, and R. L. Workman, Pion photoproduction on the nucleon in the quark model, Phys. Rev. C **65**, 065204 (2002).
[51] A. J. Arifi, D. Suenaga, and A. Hosaka, Relativistic corrections to decays of heavy baryons in the quark model, Phys. Rev. D **103**, 094003 (2021).
[52] A. J. Arifi, D. Suenaga, A. Hosaka, and Y. Oh, Strong decays of multistrangeness baryon resonances in the quark model, Phys. Rev. D **105**, 094006 (2022).
[53] H. W. Fearing, G. I. Poulis, and S. Scherer, Effective Hamiltonians with relativistic corrections. 1. The Foldy-Wouthuysen transformation versus the direct Pauli reduction, Nucl. Phys. **A570**, 657 (1994).
[54] L. L. Foldy and S. A. Wouthuysen, On the Dirac theory of spin 1/2 particle and its nonrelativistic limit, Phys. Rev. **78**, 29 (1950).
[55] J. D. Bjorken and S. D. Drell, *Relativistic Quantum Mechanics* (McGraw-Hill, New York, 1965), ISBN 978-0-07-005493-6.
[56] W. Greiner, *Relativistic Quantum Mechanics: Wave Equations* (Springer, New York, 1990).
[57] T. Kubota and K. Ohta, Relativistic corrections to the baryon resonance photoexcitation amplitudes in the quark model, Phys. Lett. **65B**, 374 (1976).
[58] X. H. Zhong and Q. Zhao, Charmed baryon strong decays in a chiral quark model, Phys. Rev. D **77**, 074008 (2008).
[59] K. L. Wang, Y. X. Yao, X. H. Zhong, and Q. Zhao, Strong and radiative decays of the low-lying S- and P-wave singly heavy baryons, Phys. Rev. D **96**, 116016 (2017).
[60] Y. X. Yao, K. L. Wang, and X. H. Zhong, Strong and radiative decays of the low-lying D-wave singly heavy baryons, Phys. Rev. D **98**, 076015 (2018).
[61] K. L. Wang, L. Y. Xiao, X. H. Zhong, and Q. Zhao, Understanding the newly observed Ω_c states through their decays, Phys. Rev. D **95**, 116010 (2017).
[62] L. Y. Xiao and X. H. Zhong, Possible interpretation of the newly observed $\Omega(2012)$ state, Phys. Rev. D **98**, 034004 (2018).
[63] K. L. Wang, Q. F. Lü, and X. H. Zhong, Interpretation of the newly observed $\Sigma_b(6097)^{\pm}$ and $\Xi_b(6227)^-$ states as the P-wave bottom baryons, Phys. Rev. D **99**, 014011 (2019).
[64] K. L. Wang, Q. F. Lü, and X. H. Zhong, Interpretation of the newly observed $\Lambda_b(6146)^0$ and $\Lambda_b(6152)^0$ states in a chiral quark model, Phys. Rev. D **100**, 114035 (2019).
[65] M. S. Liu, K. L. Wang, Q. F. Lü, and X. H. Zhong, Ω baryon spectrum and their decays in a constituent quark model, Phys. Rev. D **101**, 016002 (2020).
[66] L. Y. Xiao, K. L. Wang, M. S. Liu, and X. H. Zhong, Possible interpretation of the newly observed Ω_b states, Eur. Phys. J. C **80**, 279 (2020).
[67] K. L. Wang, L. Y. Xiao, and X. H. Zhong, Understanding the newly observed Ξ_c^0 states through their decays, Phys. Rev. D **102**, 034029 (2020).
[68] L. Y. Xiao and X. H. Zhong, Toward establishing the low-lying P-wave Σ_b states, Phys. Rev. D **102**, 014009 (2020).
[69] W. J. Wang, Y. H. Zhou, L. Y. Xiao, and X. H. Zhong, $1D$-wave bottom-strange baryons and possible interpretation of $\Xi_b(6327)^0$ and $\Xi_b(6333)^0$, Phys. Rev. D **105**, 074008 (2022).

[70] H. H. Zhong, R. H. Ni, M. Y. Chen, X. H. Zhong, and J. J. Xie, Further study of $\Omega^*|1P^-_{3/2}\rangle$ within a chiral quark model, Chin. Phys. C **47**, 063104 (2023).

[71] W. J. Wang, L. Y. Xiao, and X. H. Zhong, Strong decays of the low-lying ρ-mode 1P-wave singly heavy baryons, Phys. Rev. D **106**, 074020 (2022).

[72] B. Silvestre- Brac and C. Gignoux, Unitary effects in spin orbit splitting of P wave baryons, Phys. Rev. D **43**, 3699 (1991).

[73] Z. Yang, G. J. Wang, J. J. Wu, M. Oka, and S. L. Zhu, Novel coupled channel framework connecting the quark model and lattice QCD for the near-threshold Ds states, Phys. Rev. Lett. **128**, 112001 (2022).

[74] P. G. Ortega, J. Segovia, D. R. Entem, and F. Fernandez, Molecular components in P-wave charmed-strange mesons, Phys. Rev. D **94**, 074037 (2016).

[75] P. G. Ortega, J. Segovia, D. R. Entem, and F. Fernández, Threshold effects in P-wave bottom-strange mesons, Phys. Rev. D **95**, 034010 (2017).

[76] Z. Yang, G. J. Wang, J. J. Wu, M. Oka, and S. L. Zhu, The investigations of the P-wave B_s states combining quark model and lattice QCD in the coupled channel framework, J. High Energy Phys. 01 (2023) 058.

[77] K. Brauer, A. Faessler, F. Fernandez, and K. Shimizu, Nucleon-nucleon interaction in a quark model with pions, Nucl. Phys. **A507**, 599 (1990).

[78] Z. Y. Zhang, A. Faessler, U. Straub, and L. Y. Glozman, The baryon baryon interaction in a modified quark model, Nucl. Phys. **A578**, 573 (1994).

[79] Y. W. Yu, Z. Y. Zhang, P. N. Shen, and L. R. Dai, Quark quark potential from chiral symmetry, Phys. Rev. C **52**, 3393 (1995).

[80] A. Valcarce, H. Garcilazo, F. Fernandez, and P. Gonzalez, Quark-model study of few-baryon systems, Rep. Prog. Phys. **68**, 965 (2005).

[81] A. Valcarce, H. Garcilazo, and J. Vijande, Constituent quark model study of light- and strange-baryon spectra, Phys. Rev. C **72**, 025206 (2005).

[82] Y. B. Dai, X. Q. Li, S. L. Zhu, and Y. B. Zuo, Contribution of DK continuum in the QCD sum rule for $D_{sJ}(2317)$, Eur. Phys. J. C **55**, 249 (2008).

[83] E. van Beveren and G. Rupp, Observed $D_s(2317)$ and tentative $D(2100-2300)$ as the charmed cousins of the light scalar nonet, Phys. Rev. Lett. **91**, 012003 (2003).

[84] M. Albaladejo, P. Fernandez-Soler, F. K. Guo, and J. Nieves, Two-pole structure of the $D_0^*(2400)$, Phys. Lett. B **767**, 465 (2017).

[85] M. L. Du, M. Albaladejo, P. Fernández-Soler, F. K. Guo, C. Hanhart, U. G. Meißner, J. Nieves, and D. L. Yao, Towards a new paradigm for heavy-light meson spectroscopy, Phys. Rev. D **98**, 094018 (2018).

[86] M. L. Du, F. K. Guo, C. Hanhart, B. Kubis, and U. G. Meißner, Where is the lightest charmed scalar meson?, Phys. Rev. Lett. **126**, 192001 (2021).

[87] W. A. Bardeen, E. J. Eichten, and C. T. Hill, Chiral multiplets of heavy—light mesons, Phys. Rev. D **68**, 054024 (2003).

[88] L. Gayer, N. Lang, S. M. Ryan, D. Tims, C. E. Thomas, and D. J. Wilson (Hadron Spectrum Collaboration), Isospin-1/2 $D\pi$ scattering and the lightest D_0^* resonance from lattice QCD, J. High Energy Phys. 07 (2021) 123.

[89] R. Aaij *et al.* (LHCb Collaboration), First observation and amplitude analysis of the $B^- \to D^+K^-\pi^-$ decay, Phys. Rev. D **91**, 092002 (2015); **93**, 119901(E) (2016).

[90] I. Woo Lee and T. Lee, Why there is no spin-orbit inversion in heavy-light mesons?, Phys. Rev. D **76**, 014017 (2007).

[91] J. Vijande, A. Valcarce, and F. Fernandez, B meson spectroscopy, Phys. Rev. D **77**, 017501 (2008).

[92] S. L. Zhu and Y. B. Dai, The effect of $B\pi$ continuum in the QCD sum rules for the $(0^+, 1^+)$ heavy meson doublet in HQET, Mod. Phys. Lett. A **14**, 2367 (1999).

[93] C. B. Lang, D. Mohler, S. Prelovsek, and R. M. Woloshyn, Predicting positive parity B_s mesons from lattice QCD, Phys. Lett. B **750**, 17 (2015).

[94] E. B. Gregory, C. T. H. Davies, I. D. Kendall, J. Koponen, K. Wong, E. Follana, E. Gamiz, G. P. Lepage, E. H. Muller, H. Na *et al.*, Precise B, B_s and B_c meson spectroscopy from full lattice QCD, Phys. Rev. D **83**, 014506 (2011).

[95] H. Y. Cheng and F. S. Yu, Near mass degeneracy in the scalar meson sector: Implications for $B^*_{(s)0}$ and $B'_{(s)1}$ mesons, Phys. Rev. D **89**, 114017 (2014).

[96] H. Y. Cheng and F. S. Yu, Masses of scalar and axial-vector B mesons revisited, Eur. Phys. J. C **77**, 668 (2017).

[97] M. Albaladejo, P. Fernandez-Soler, J. Nieves, and P. G. Ortega, Lowest-lying even-parity $\bar{B}_s$ mesons: Heavy-quark spin-flavor symmetry, chiral dynamics, and constituent quark-model bare masses, Eur. Phys. J. C **77**, 170 (2017).

[98] F. K. Guo, P. N. Shen, and H. C. Chiang, Dynamically generated 1^+ heavy mesons, Phys. Lett. B **647**, 133 (2007).

[99] F. K. Guo, P. N. Shen, H. C. Chiang, R. G. Ping, and B. S. Zou, Dynamically generated 0^+ heavy mesons in a heavy chiral unitary approach, Phys. Lett. B **641**, 278 (2006).

[100] G. L. Yu and Z. G. Wang, Analysis of the excited bottom and bottom-strange states $B_1(5721)$, $B_2^*(5747)$, $B_{s1}(5830)$, $B_{s2}^*(5840)$, $B_J(5840)$ and $B_J(5970)$ in B meson family, Chin. Phys. C **44**, 033103 (2020).

[101] R. Aaij *et al.* (LHCb Collaboration), Observation of new excited B_s^0 states, Eur. Phys. J. C **81**, 601 (2021).

[102] E. Eichten, K. Gottfried, T. Kinoshita, K. D. Lane, and T. M. Yan, Charmonium: The model, Phys. Rev. D **17**, 3090 (1978); **21**, 313(E) (1980).

[103] S. Godfrey and N. Isgur, Mesons in a relativized quark model with chromodynamics, Phys. Rev. D **32**, 189 (1985).

[104] T. Barnes, S. Godfrey, and E. S. Swanson, Higher charmonia, Phys. Rev. D **72**, 054026 (2005).

[105] E. Hiyama, Y. Kino, and M. Kamimura, Gaussian expansion method for few-body systems, Prog. Part. Nucl. Phys. **51**, 223 (2003).

[106] J. Zeng, J. W. Van Orden, and W. Roberts, Heavy mesons in a relativistic model, Phys. Rev. D **52**, 5229 (1995).

[107] W. J. Deng, H. Liu, L. C. Gui, and X. H. Zhong, Spectrum and electromagnetic transitions of bottomonium, Phys. Rev. D **95**, 074002 (2017).

[108] W. J. Deng, H. Liu, L. C. Gui, and X. H. Zhong, Charmonium spectrum and their electromagnetic transitions with higher multipole contributions, Phys. Rev. D **95**, 034026 (2017).

[109] Q. Li, M. S. Liu, L. S. Lu, Q. F. Lü, L. C. Gui, and X. H. Zhong, Excited bottom-charmed mesons in a nonrelativistic quark model, Phys. Rev. D **99**, 096020 (2019).

[110] Q. Li, L. C. Gui, M. S. Liu, Q. F. Lü, and X. H. Zhong, Mass spectrum and strong decays of strangeonium in a constituent quark model, Chin. Phys. C **45**, 023116 (2021).